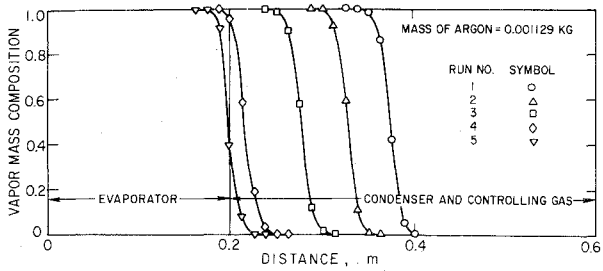

Fig. 3 Axial sodium-vapor mass composition variation along the vapor-liquid interface of the gas-loaded heat pipe.

transfer coefficients in condenser and evaporator respectively. From these results, the minimum heat transfer rate for the heat pipe under study is found to be about 200 w, and at heat transfer rates below this level a continuous temperature drop occurs along the heat pipe.

Similar to the simple heat pipe case, a cylindrical heat pipe with sodium as the working fluid and argon as the controlling gas is selected for the analysis.[7] Five cases of the sodium-argon gas-loaded heat pipe are analyzed. In these cases, the rate of heat transfer through the system is lowered in such a way that the constant mass of argon occupies an increasing length of the heat pipe condenser section and eventually enters the heat pipe evaporator section in Case No. 5. Table 2 gives the primary

Table 2 Primary information on the five sodium-argon gas-loaded heat pipe cases

Case No.	$T_{ac}(K)$	$T_{ae}(K)$	$T_o(K)$	$r_o(m)$	$L(m)$	H_c $(Wm^{-2}K^{-1})$	H_e
1	400	1000	900	0.025	0.6	32	159
2	400	944	873	0.025	0.6	32	159
3	400	905	859	0.025	0.6	32	159
4	400	870	848	0.025	0.6	32	159
5	400	851	842	0.025	0.6	32	159

information about the cases studied while Figs. 2 and 3 demonstrate the axial temperature and sodium vapor mass composition variations along the heat pipe vapor-liquid interface. The minimum heat transfer rate limit is about 250 watts here as demonstrated in Figs. 2 and 3. The profiles in Figs. 1–3 are obtained as mentioned before, by neglecting the axial heat conduction through the heat pipe wall and the liquid-wick matrix. Obviously, when this conduction contribution is taken into consideration, the minimum heat transfer limit will be much higher, and its importance in actual design consideration cannot be overlooked.

References

[1] Cotter, T. P., "Theory of Heat Pipes," Rept. LA-3246-MS, March 1965, Los Alamos Scientific Lab., Los Alamos, New Mex.

[2] Kemme, J. E., "Heat Pipe Design Considerations," Rept. LA-4221-MS, August 1966, Los Alamos Scientific Lab. Los Alamos, New Mex.

[3] Levy, E. K., "Theoretical Investigation of Heat Pipes Operating at Low Vapor Pressures," *Journal of Engineering for Industry*, Vol. 90, 1968, pp. 547–552.

[4] Busse, C. A., "Theory of the Ultimate Heat Transfer Limit of Cylindrical Heat Pipes," *International Journal of Heat and Mass Transfer*, Vol. 16, 1973, pp. 169–186.

[5] Marcus, B. D., Fleischman, C. L., and Edwards, D. K., "Diffusion Freeze-out in Gas-Loaded Heat Pipes," ASME Paper 72-WA/HT-33, 1972.

[6] Tien, C. L., and Rohani, A. R., "Analysis of the Effects of Vapor Pressure Drop on Heat Pipe Performance," *International Journal of Heat and Mass Transfer*, Vol. 17, 1974, pp. 61–67.

[7] Rohani, A. R., and Tien, C. L., "Steady Two-Dimensional Heat and Mass Transfer in the Vapor-Gas Region of a Gas-Loaded Heat Pipe," *Journal of Heat Transfer*, Vol. 95, 1973, pp. 337–382.

[8] Cotter, T. P., "Heat Pipe Startup Dynamics," *1967 IEEE Conference Record of the Thermionic Conversion Specialist Conference*, 1967, pp. 344–348.

[9] Gosman, A. D., Pun, W. M., Runchal, A. K., Spalding, D. B. and Wolfstein, M., *Heat and Mass Transfer in Recirculating Flows*, Academic Press, New York, 1969.

Variable Time Step Method for Determining Plastic Stress Reflections from Boundaries

HYMAN GARNET* AND HARRY ARMEN†
Grumman Aerospace Corporation, Bethpage, N.Y.

IT is the purpose of this Note to call attention to the advantages of the use of a variable time step direct integration method, in conjunction with a finite element analysis, for obtaining accurate results for elasto-plastic wave propagation, including reflections from fixed boundaries.

Recently, increased interest has been shown in the application of finite element analyses to problems in structural dynamics. An important role in such procedures is the appropriate use of a direct integration method to handle the time dependence. The more popular schemes employed have been Houbolt's, Newmark-Beta, central difference, and Wilson's methods. These procedures have been surveyed in a number of publications, for example, by Nickell[1] and the present authors.[2] These procedures all involve the use of a constant time step.

The present authors applied a number of direct integration techniques to the finite element analysis of a rod experiencing elastic and elasto-plastic wave propagation effects, either from an applied step pulse, or from a constant velocity impact into a rigid barrier.[2] After completion of the investigation, it was concluded that constant time step procedures, while capable of being adjusted to converge to acceptable results, were inappropriate to many practical problems, in particular to the increasingly important area of crashworthiness. The problem of selecting a constant time step, which would lead to convergent results is computationally equivalent to "flying" a vehicle, crashing it, and analyzing it several times until a time step is found that produces satisfactory convergence. This need for duplication of analysis is eliminated by the use of variable time step procedures, in which the time step may be varied at different instants to reflect the dynamic behavior of the structure, i.e., the time increment is increased during a slowly varying portion of the response, and decreased during a rapidly varying portion of the response. Thus, stability, accuracy, and efficiency requirements are met by built-in procedures.

In this Note, the authors draw on results obtained by them in Ref. 1, and more recently, to support the feasibility of applying a variable time step procedure to finite element structural dynamic analysis. The procedure referred to is a Grumman-developed version of the modified Adams method.[3] It has been applied to a variety of significant aerospace structural dynamics problems, for example, as listed in Refs. 4 and 5. Recently, the present authors have employed this variable time step procedure to obtain accurate predicted results for elasto-plastic wave propagation, including the case of waves reflected from boundaries. The method employs Taylor series expansions to obtain predictor-corrector expressions, truncated to difference form, of the solution to a first-order system of

Received July 31, 1974; revision received September 18, 1974.
Index category: Aircraft Structural Design (Including Loads).

* Research Scientist, Research Department.
† Head, Applied Mechanics Branch. Member AIAA.

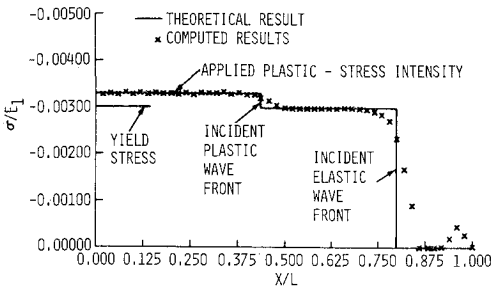

Fig. 1 Stress response when elastic wave has travelled 0.8 the length of the bar ($E_2/E_1 = 0.1$).

nonlinear equations. The corresponding second-order system of equations of motion is employed to construct the corrector expression. The procedure is described in detail in Ref. 3.

A bilinear stress-strain law was assumed and a constant-strain finite element rod and its associated consistent mass matrix was employed. Results (Figs. 1 and 2) are presented in nondimensional form for the case of a step pulse applied to the free end of a built-in bar. The ordinates represent stress divided by the elastic Young's modulus; the abscissas denote non-dimensional distances. These distances are actual distances from the free end, divided by the length of the bar.

Figure 1 shows the elasto-plastic response, when the elastic waves has traveled 0.8 the length of the bar. The theoretical value of the response may, in this case, be obtained by methods presented by Donnell.[6] As can be seen, the step plastic and elastic wave fronts are approximated by ramps. This sort of approximation is to be expected from a numerical procedure and represents a fair approximation to the position of the wave front. At the same time it gives an excellent prediction of the stress level.

Depicted in Fig. 2 is the stress response after the precursor wave front, traveling at the elastic wave speed, but possessing yield stress intensity, has reflected from the fixed end as a plastic wave. This response corresponds to a time when an elastic wave would have returned 0.4 the length of the bar. Shown are the theoretical positions of the incident and reflected plastic waves, and the theoretical value of the reflected plastic stress intensity. The determination of the reflected wave properties is discussed in the appendix.

These results, and others obtained by the authors (as mentioned in greater detail in the appendix), are encouraging because the strains in the reflecteu plastic waves represent a fair-sized jump with respect to that of the incident wave. The indications are that the Grumman-developed version of the modified Adams procedure is a viable direct time integration code, capable of handling dynamic elasto-plastic analyses. Similar success may be anticipated in multidimensional cases.

Appendix: Reflected Plastic Waves

It is well known[6] that in the case of a one dimensional bar, when the intensity of an incident compressive wave, σ_i, is less

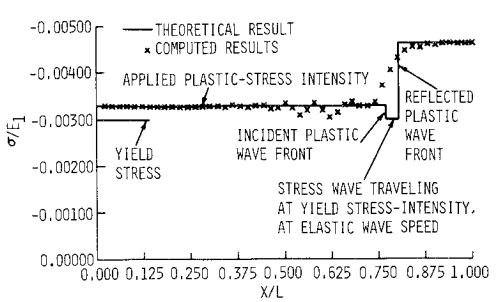

Fig. 2 Stress response after elastic wave front has undergone plastic reflection ($E_2/E_1 = 0.1$).

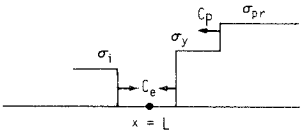

Fig. 3 Waves entering into the construction of the plastic reflection.

than half the yield stress, i.e., $\sigma_i \leqq \sigma_y/2$, reflection from a fixed boundary occurs, with the intensity of the reflected wave, σ_r, equal to twice that of the incident wave, i.e., $\sigma_r = 2\sigma_i$. This is not true when $\sigma_i > \sigma_y/2$, for plastic effects result, and the situation is more complex. Graphical methods have been presented by DeJuhasz[7] and Davids and Kumar[8] for dealing with bars stressed above the elastic range. A procedure suggested by these approaches is presented now for determining the intensity of the reflected compressive wave when $\sigma_i > \sigma_y/2$.

Consider a free body diagram (including inertia forces) of an element of a uniform rod of constant cross section, A, and density, ρ. Let the symbols σ and v denote stress and particle velocities, respectively, then D'Lambert's principle yields

$$\rho(dv/dt) = d\sigma/dx \tag{A1}$$

If c is the speed of wave propagation, during the interval dt, then $dx = c\,dt$. This results in

$$dv = d\sigma/\rho c \tag{A2}$$

Equation (A2) describes the change in particle velocity during the time interval, dt.

Following Ref. 7, the solution is constructed from the following components: 1) an incident elastic wave traveling with intensity σ_i, $\sigma_y/2 < \sigma_i \leqq \sigma_y$; 2) a wave traveling in the direction opposite that of the incident wave, at yield stress intensity and elastic speed of propagation, c_e; and 3) a plastic wave also traveling opposite to the incident wave, at plastic speed of propagation, c_p, and at as yet undetermined stress intensity, σ_{pr}. Figure 3 depicts this situation.

By ensuring that the total particle velocity v_T resulting from these contributions is zero, the boundary condition for a fixed end is enforced, and from this condition the value of σ_{pr}, the intensity of the reflected plastic wave, may be computed. From the relation (A2), and the bilinear stress-strain law, the sum of these contributions is

$$\int_0^{\sigma_i} d\sigma/\rho c_e - \int_{\sigma_i}^{\sigma_y} d\sigma/\rho c_e - \int_{\sigma_y}^{\sigma_{pr}} d\sigma/\rho c_p = 0 \tag{A3}$$

in which c_e and c_p are the elastic and plastic wave speeds, respectively, and are given by

$$c_e = (E_1/\rho)^{1/2}, \qquad c_p = (E_2/\rho)^{1/2} \tag{A4}$$

where E_1 and E_2 are the slopes of the elastic and plastic portions of the bilinear stress-strain curves, respectively.

After the integrations are carried out, the following result is obtained for σ_{pr}

$$\sigma_{pr} = \sigma_y + (c_p/c_e)[2\sigma_i - \sigma_y] \tag{A5}$$

By letting $\bar{\sigma} = \sigma/E_1$, and using Eq. (A4), Eq. (A5) is given in nondimensional form as

$$\bar{\sigma}_p = [1.0 - (E_2/E_1)^{1/2}]e_y + 2(E_2/E_1)^{1/2}\bar{\sigma}_i \tag{A6}$$

in which use has been made of the fact that $\bar{\sigma}_y = e_y$, the yield strain. The results shown in Figs. 1 and 2 were obtained by use of Eq. (A6).

The present authors[9] have also investigated more complex cases. For example, the case which results when the reflected plastic wave interacts with the incident plastic wave, and also the case which results when the incident plastic wave reflects from the fixed boundary. Analytical expressions were derived and good agreement with computational results was obtained.

References

[1] Nickell, R. E., "Direct Integration Methods in Structural Dynamics," *Journal of the Engineering Mechanics Division, (EM2, Proceedings of the American Society of Civil Engineers)*, April 1973, pp. 303–317.

[2] Garnet, H. and Armen, H., *Evaluation of Numerical Time Integration Methods as Applied to Elastic-Plastic Dynamic Problems Involving Wave Propagation*, Rept. RE-475, March 1974, Research Dept., Grumman Aircraft Corp., Bethpage, N.Y.

[3] Stoodley, G. R. and Ball, D. J., *Mathematical Background of Two Numerical Integration Techniques for Ordinary Differential Equations*, Memo. RM-192, Oct. 1961, Research Dept., Grumman Aircraft Corp., Bethpage, N.Y.

[4] Mantus, M., Lerner, E., and Elkins, W., "Landing Dynamics of the Lunar Excursion Module (Method of Analysis)," Rept. LED-520-6A, Revised April 10, 1967, Grumman Aircraft Corp., Bethpage, N.Y.

[5] Lerner, E. and Mantus, M., "Dynamics of Unsymmetric Landing," Rept. ADR 02-10-10-62-1, Jan. 1963, Grumman Aircraft Corp., Bethpage, N.Y.

[6] Donnell, L. H., "Longitudinal Wave Transmission and Impact," *Transactions of the ASME*, Vol, 52, 1930, pp. 153–167.

[7] DeJuhasz, K. J., "Graphical Analysis of Impact of Bars Stressed Above the Elastic Range," *Journal of the Franklin Institute*, Vol. 248, No. 2, Aug. 1949, pp. 113–142.

[8] Davids, N. and Kumar, S., "A Contour Method for One Dimensional Pulse Propagation in Elastic-Plastic Materials," *Proceedings of the Third U.S. National Congress of Applied Mechanics*, Brown University, Providence, R.I., 1958, pp. 502–512.

[9] Garnet, H. and Armen, H., *One Dimensional Elastic-Plastic Wave Propagation and Boundary Reflections*, Memo, Grumman Research Department, Bethpage, N.Y. (in preparation).

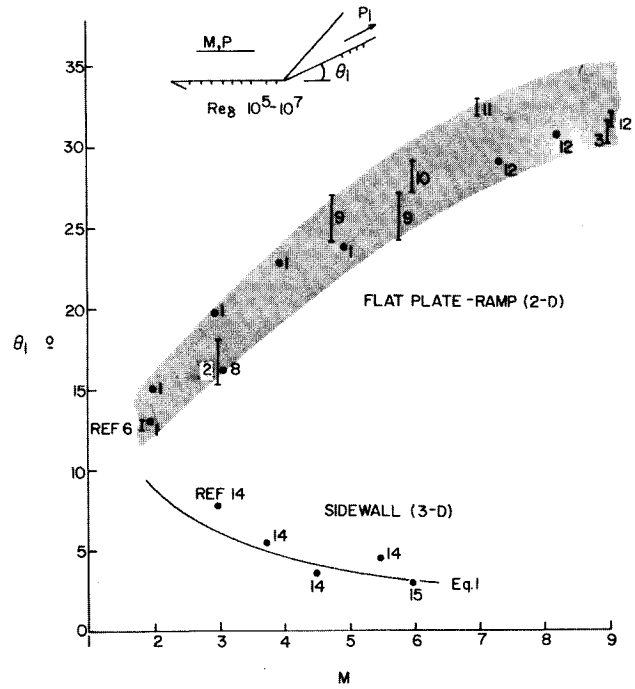

Fig. 2 Incipient separation angle.

Comparison of Shock-Induced Two- and Three-Dimensional Incipient Turbulent Separation

R. H. KORKEGI*
Aerospace Research Laboratories, Wright-Patterson Air Force Base, Ohio

Introduction

SHOCK waves resulting from sudden compressions in axial corners or in rectangular ducts, interact two-dimensionally with the boundary layer on the compression surface and three-dimensionally (skewed or glancing shock) with the layer on the adjacent surface. The configuration is illustrated in Fig. 1. It is typical of the flow in "two-dimensional" supersonic diffusers.

The purpose of this Note is to present available quantitative data for conditions of incipient separation of turbulent boundary layers due to two-dimensional and skewed shock wave interactions and thus show that separation will occur much earlier for the latter than for the former types of interaction. This information is designed to bring together what is presently known about two and three-dimensional shock wave-turbulent interactions; however, much more data is needed for in-depth knowledge and for defining characteristics of separation.

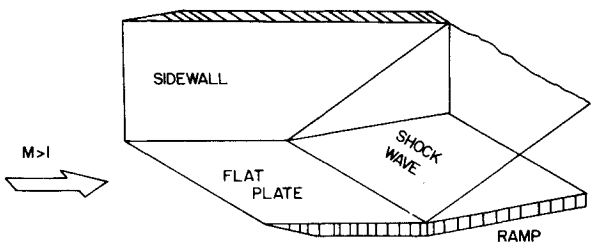

Fig. 1

Received September 10, 1974.
Index categories: Boundary Layers and Convective Heat Transfer—Turbulent; Supersonic and Hypersonic Flows.

* Director, Theoretical Aerodynamics Research Laboratory. Associate Fellow AIAA.

Incipient Separation Data

In order to avoid the possibility of transitional effects, only data corresponding to $Re_\delta > 10^5$ are considered. According to experimental evidence, the compression angle θ_i for two-dimensional incipient turbulent boundary-layer separation first decreases, then increases slowly[1,2] with increasing Re_δ; decreasing wall temperature also results in some increase in θ_i.[3] However, these variations are considerably smaller than for the laminar case.[4]

For incipient turbulent boundary-layer separation due to a skewed shock wave, the present author[5] has shown that existing data up to $M = 3.5$ correlate according to

$$M\theta_i = 0.3 \text{ (radians)} \tag{1}$$

Corresponding to which the pressure rise across the shock wave is $P_i/p = 1.50$ independent of M.

Incipient separation data[1-3,6-15] for both two-dimensional and skewed shock wave-turbulent boundary-layer interactions are shown in Fig. 2. The numerals indicate references. The vertical lines indicate data over a wide range of Reynolds numbers and/or limits of accuracy, if known. Included in Fig. 2 for the three-dimensional case are new data points from Neumann and Token[14] up to $M = 5.5$ and one from Law[15] which tend to confirm the trend of the correlation. Additional data on three-dimensional interactions at $M = 5.9$ by Goldberg[16] is not included because the incipient separation angle could not be determined with sufficient accuracy.

The pressure rise for incipient separation corresponding to Fig. 2 is shown in Fig. 3, along with two empirical correlations for the two dimensional case, adequate for rough estimates, in which no account is taken of the effect of Reynolds number and wall temperature variations as these are not large to a first order. The correlations are:

$$C_{p_i} = 0.43 \quad \text{or} \quad p_i/p = 1 + 0.3M^2 \qquad M \lesssim 4.5 \tag{2}$$

and

$$p_i/p = 0.17M^{2.5} \qquad M \gtrsim 4.5 \tag{3}$$